

## Eccentricity with non-parallel axes of symmetry and rotation – movement of gear teeth along the axis of rotation

Łukasz Jedliński<sup>1</sup> 

<sup>1</sup> Lublin University of Technology, ul. Nadbystrzycka 38 D 20-618 Lublin, Poland

\* Corresponding author's e-mail: l.jedlinski@pollub.pl

### ABSTRACT

The problem of gear eccentricity is more and more often considered and developed in simulation models. Eccentricity is unavoidable due to finite manufacturing accuracy and assembly process and thus can only be minimised. Eccentricity can have a significant impact on dynamics primarily due to its effect on gear stiffness and teeth position. Previous models of gear eccentricity have dealt with parallel axes. When considering the problem of eccentricity with non-parallel axes of symmetry and rotation, one must take into account new phenomena that occur. For a case of eccentricity with non-parallel axes, such phenomenon is the axial displacement of gear teeth, the occurrence of which generates a friction force along the axis of rotation of the gear. The main objective of this study is therefore to develop a model that would take the axial movement of gear teeth into account. To this end, the kinematic parameters of this movement, including displacement, velocity and acceleration, are determined in a selected plane. The developed models should contribute to increased accuracy of modelling gear operation and occurring phenomena. Analysing teeth friction in occurrence of eccentricity with non-parallel axes must include axial movement of teeth to receive accurate results. In the case of helical gears the influence on dynamic behaviour is even greater because of direct influence of position of contact point.

**Keywords:** non-parallel eccentricity, axial friction force, spur gear axial movement, base circle reference, centre distance.

### INTRODUCTION

Previous studies on gears have investigated various aspects of their operation. One of the main causes of vibration and noise is time-varying mesh stiffness (TVMS) which depends on many factors. As a result, there has been in a continuing strong interest in the study of TVMS. A study [1] proposed an analytical model for accurate TVMS calculation for spiral bevel gears. A study [2] investigated the mesh stiffness of planetary gears, while in [3] it was investigated for spur gears.

Other research works devoted to gears focused on problems such as extended tooth contact due to gear elasticity [4], the centrifugal effect on mesh stiffness [5, 6], the effects of gear tooth crack [7, 8] and spalling [9] on gear mesh stiffness, the analysis of load distribution in planetary

gears [10], as well as the impact of eccentricity on power losses [11]. Although these are the main research directions, they are not the only ones, because the current trend is to investigate many aspects within a single study relating to gears.

Eccentricity in different types of gears and its effect on gear dynamics is a more and more widely studied problem. It always occurs as a result of limited manufacturing accuracy and assembly process. Models have been developed for planetary gears, where the eccentricity error primarily affects planets [12] or planets and a sun [13]. As for cylindrical gears, spur gears [14] and helical gears [15] are considered. Eccentricity affects, among other things, gear spacing and pressure angle, which translates into a change in contact ratio and, consequently, gear mesh stiffness and teeth position. It therefore has a significant impact on gear dynamics.

Previous studies investigated the eccentricity model relating to a case where the axis of symmetry of the gear was parallel relative to the axis of rotation [12, 14–16]. This is the basic variant and the simplest to analyse, yet it is representative of a smaller proportion of cases occurring in reality. In the general case of eccentricity, the axis of symmetry of the gear neither overlaps with the axis of rotation, nor it is parallel to this axis. By dividing the gear into segments, we can determine the centres of gravity for these segments. The trajectories of the centres of gravity of the segments will form circles of varying diameters. Still, the general eccentricity case requires determining the radius of eccentricity and its location, which is not an easy task. A study [17] was the first to have investigated such case and to have proposed a method for determining these eccentricity parameters.

The meshing of gears for a case of eccentricity with non-parallel axes is more complicated than for parallel axes. There is an additional movement of the teeth along the axis of rotation. Since the position of the gear teeth for eccentricity with non-parallel axes depends on their contact point along the face width, the simulation of such case requires the use of a segmented gear model for more accurate representation. To facilitate analyses of such cases, the main objective of this study is to determine the parameters of movement along the axis of rotation – in other words, to establish relationships describing the displacement, velocity and acceleration of gears in any plane.

This work offers an extension of the model proposed in [17]. For validation of the obtained equations for kinematic parameters, results will be presented for displacement, velocity and acceleration along the axis of rotation for two different cases of eccentricity. The occurrence of motion along the axis of rotation makes the determination of friction force difficult. Previous studies focused on the friction force only along the off-line of action (OLOA). For eccentricity with non-parallel axes, the total friction force consists of a force component acting in the OLOA direction and a force component that is parallel to the axis of rotation. Hence, additional simulations were performed to determine the friction force components and vibrations along the pinion's axis of rotation.

## DETERMINATION OF THE KINEMATIC PARAMETERS OF AXIAL DISPLACEMENT $z_o$

Manufacturing and assembly errors or wear may cause the axis of symmetry of the gear to be displaced in relation to the axis of rotation. The distance of the axis of symmetry of the gear in relation to the axis of rotation in the bearing plane is known as eccentricity. If the axes are not parallel, there is an axial displacement of the gear during gear rotation. This results in axial movement of the teeth, for which, under normal operating conditions, relative movement in the axial direction does not occur. The movement of the gear teeth in the axial direction causes the teeth to slide and thus generates the friction force.

### Determination of the axial displacement $z_o$ in a plane perpendicular to the minimal distance

The axial displacement of the gear teeth with eccentricity is shown in Figure 1. The plane in which the distance  $z_o$  is determined is perpendicular to the minimum distance and passes through the centre of the gear. The gear is rotated by an angle  $\varphi_l$  with respect to the theoretical position. The determination of the distance  $z_o$  for this case is simple and made in accordance with the relation:

$$z_o = r_w \sin \varphi_l \tag{1}$$

where: the distance  $z_o$  is determined on the rolling radius  $r_w$  that is parallel to the axis of rotation.

The above method of  $z_o$  determination was developed for a plane perpendicular to the minimum distance. The axial displacement  $z_o$  reaches its maximum value for this case. However, the same approach cannot be employed to determine the distance in any plane, which is a must in gear simulation.

### Determination of the axial displacement $z_o$ in any plane

Figure 2 shows the spatial view of the position of a gear with eccentricity radii  $r_{e1}$  and  $r_{e2}$  defined in the bearing planes. The gear with a rolling radius  $r_w$  is denoted by the blue circle (plane  $\pi_b$ ). The axis of symmetry of the gear is located in the circles described by eccentricity radii  $r_{e1}$  and  $r_{e2}$ .

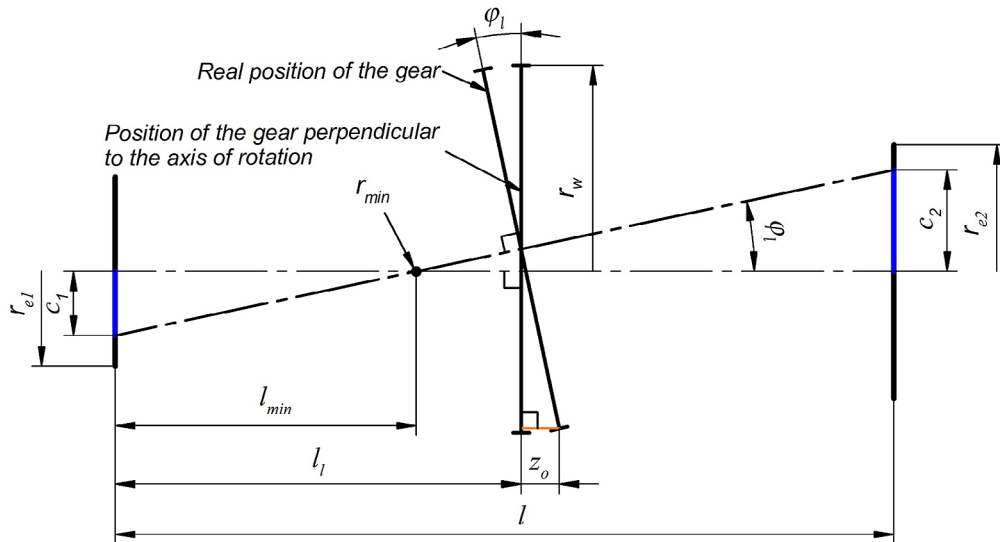


Figure 1. Axial displacement  $z_o$  of gear teeth due to eccentricity

The green circle (plane  $\pi_a$ ) represents the position of the gear with eccentricity perpendicular to the axis of rotation. The blue and green circles have a common centre denoted by  $O$ . The intersection of the blue and green circles (as well as of the planes  $\pi_b$  and  $\pi_a$ ) forms a common edge through which an axis  $R_{min}$  is drawn. The position of both the  $R_{min}$  axis and the minimum distance  $r_{min}$  depends on the axes of symmetry and rotation of the gear. The  $R_{min}$  axis is always parallel to the minimum distance  $r_{min}$ . The determination of the minimum distance, its position and other eccentricity-related quantities is discussed in [17].

A plane  $\pi$  is defined on which the distance  $x_o$  should be determined. The  $\pi$  plane is parallel to the axis of rotation of the gear and passes through the point  $O$ . It is inclined relative to the  $R_{min}$  axis by any angle  $\phi_a$ . The point  $b$  is a result of the intersection of the  $\pi$  plane and the blue gear with a rolling radius  $r_w$ . By projecting the  $b$  point onto the green gear, we can calculate the distance  $z_o = |bb''|$ . To facilitate the determination of the  $z_o$  distance, the points  $b$  and  $b''$  are projected onto a plane  $\pi_l$ , which yield points  $b_l$  and  $b''_l$ . The  $\pi_l$  plane is parallel to the axis of rotation of the gear, passes through the point  $O$  and is perpendicular to

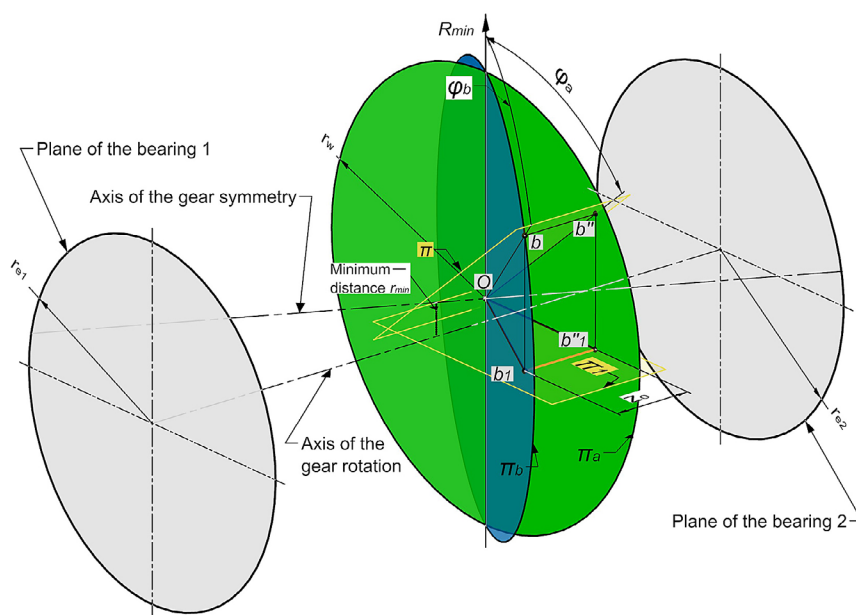


Figure 2. Axial displacement  $z_o$  of gear teeth due to eccentricity, as determined for a plane  $\pi$

the  $R_{min}$  axis. The distances between the points are therefore equal to  $z_o = |bb''| = |b_1 b_1''|$

To determine the distance  $z_o$ , it was first necessary to establish a relationship between the angles  $\varphi_a$  and  $\varphi_b$ . Figure 5 shows the gears in orthogonal projections. A point  $a$  is introduced, belonging to the green circle and the  $\pi$  plane. The  $\varphi_a$  angle lies in the green circle's plane ( $\pi_a$ ) and is defined between the arms of the angle formed by the  $R_{min}$  axis and the  $Oa$  length. Similarly, the  $\varphi_b$  angle lies in the blue circle's plane ( $\pi_b$ ) and is defined between the arms of the angle formed by the  $R_{min}$  axis and the  $Ob$  length. The points  $a$  and  $b$  lie at the same distance from the centre  $O$ . After that, a point  $c$  was introduced, and the  $b$  point was projected onto the  $\pi_a$  plane, giving rise to a point  $b'$ , as shown in Figure 3. For these points, the angle between the arms defined by the  $R_{min}$  axis and the  $Ob'$  length is equal to  $\varphi_b$ . The relationship can be written:

$$\tan \varphi_a = \frac{|cb''|}{|Oc|} \quad (2)$$

and

$$\tan \varphi_b = \frac{|cb'|}{|Oc|} \quad (3)$$

Transforming Equations 2 and 3, we get:

$$\tan \varphi_a = \frac{|cb''|}{|cb'|} \tan \varphi_b \quad (4)$$

Then, from Figure 3 b) it follows:

$$\cos \varphi_l = \frac{|cb''|}{|cb|} \quad (5)$$

It should be noted that  $|cb| = |cb'|$ , so the relationship between the angles  $\varphi_a$  and  $\varphi_b$  is:

$$\tan \varphi_a = \cos \varphi_l \tan \varphi_b \quad (6)$$

It was assumed that the  $\varphi_a$  angle is the known angle equal to pinion rotation, hence we finally get:

$$\varphi_b = \tan^{-1} \left( \frac{\tan \varphi_a}{\cos \varphi_l} \right) \quad (7)$$

Knowing the relationship in (7), we can calculate the distance  $|Ob_1|$ :

$$|Ob_1| = r_w \cos(\varphi_{bb}) \quad (8)$$

where:  $\varphi_{bb} = 90 - \varphi_b$

$$\ddot{z}_o = \frac{d^2 z}{d\varphi_a^2} = -r_w \sin \varphi_l (\tan^2(\varphi_a) + 1) \frac{\ddot{\varphi}_a \tan^3 \varphi_a - 2\dot{\varphi}_a^2 \tan^2 \varphi_a + \varphi_a^2 \cos^2 \varphi_l + 3\dot{\varphi}_a^2 \tan^2 \varphi_a \cos^2 \varphi_l + \ddot{\varphi}_a \tan \varphi_a \cos^2 \varphi_l}{\cos^4 \varphi_l \left( \frac{\tan^2(\varphi_a)}{\cos^2 \varphi_l} + 1 \right)^{5/2}} \quad (11)$$

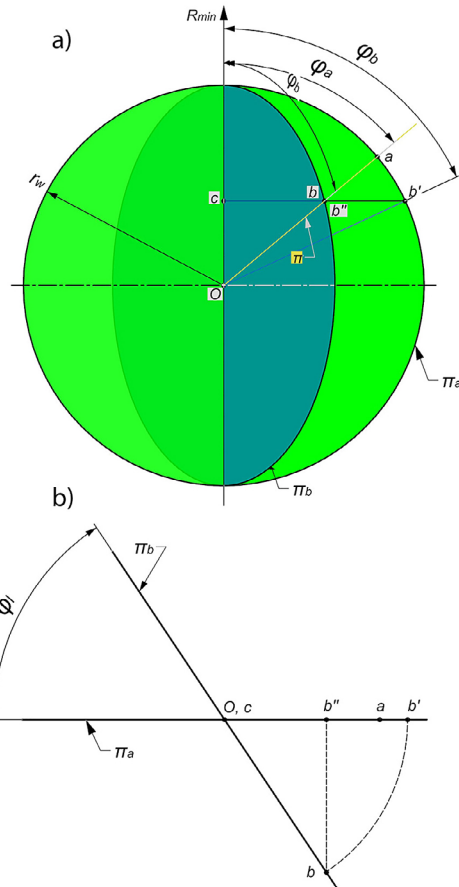


Figure 3. Relationship between the angles  $\varphi_a$  and  $\varphi_b$ . Front view a) and top view b)

Finally, the displacement  $z_o$  can be written as:

$$z_o = r_w \cos \left( 90 - \tan^{-1} \left( \frac{\tan \varphi_a}{\cos \varphi_l} \right) \right) \sin \varphi_l \quad (9)$$

Differentiating Equation 9, we obtain a relationship describing velocity:

$$\dot{z}_o = \frac{dz}{d\varphi_a} = -\dot{\varphi}_a \frac{r_w \tan \varphi_a \sin \varphi_l (\tan^2(\varphi_a) + 1)}{\cos^2 \varphi_l \left( \frac{\tan^2 \varphi_a}{\cos^2 \varphi_l} + 1 \right)^{3/2}} \quad (10)$$

and by further differentiation and transformation we obtain the equation (11) for acceleration:

The proposed research can be presented in simplified way by block diagram (Figure 4).

### DETERMINATION OF AXIAL DISPLACEMENT $z_o$ , VELOCITY $\dot{z}_o$ AND ACCELERATION $\ddot{z}_o$ FOR TWO CASES OF ECCENTRICITY

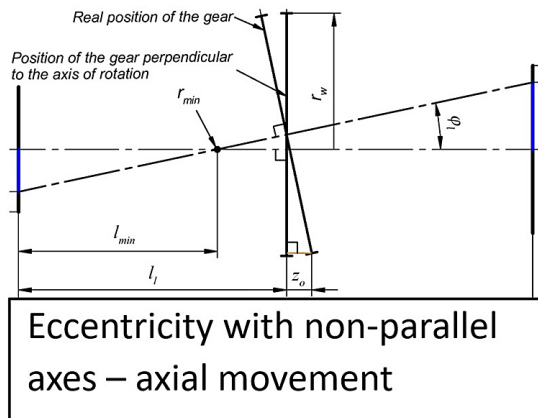
A numerical analysis was conducted to show the effect of eccentricity on the kinematic parameters associated with the axial movement of the teeth (along the axis of rotation) during mesh. The following operating conditions and gear parameters were used in the analysis:  $\pi_1 = 3000$  rpm,  $z_1 = 61$ ,  $m = 3$  mm,  $\alpha = 20^\circ$ ,  $l = 100$  mm,  $re_l = 300$   $\mu\text{m}$ . Two simulations were performed.

The first simulation was performed using the eccentricity angles  $\varphi_{e1} = 0^\circ$ ,  $\varphi_{e2} = 180^\circ$  and treating the gear as a flat element located at  $l_l = 0.5$ . For these conditions, the radius of eccentricity is  $r_{pe} = 0$ , which means that only axial movement occurs. Figure 5 shows the axial displacement  $z_o$  during one revolution of the pinion. The amplitude of the displacement is 549  $\mu\text{m}$ , and the total

displacement is almost 1.1 mm. The maximum velocity  $\dot{z}_o$  is 0.17 m/s (Figure 6) and the maximum acceleration  $\ddot{z}_o$  is 54 m/s<sup>2</sup>.

In the second simulation, the values of the eccentricity angles were changed to  $\varphi_{e1} = 50^\circ$  and  $\varphi_{e2} = 130^\circ$ . Other parameters were left unchanged. The axial displacement  $z_o$  (Figure 8) from the position 0 is 353  $\mu\text{m}$  and the total displacement is 706  $\mu\text{m}$ . The maximum value of the velocity  $\dot{z}_o$  is 0.11 m/s (Figure 9) and the maximum acceleration  $\ddot{z}_o$  is equal to 35 m/s<sup>2</sup> (Figure 10).

In both simulations, the axial displacement  $z_o$  is higher than the eccentricity radius  $r_e$ . The axial velocity  $\dot{z}_o$  is not high compared to typical slip velocities of gear teeth. On the other hand, the axial acceleration  $\ddot{z}_o$  is as high as several tens of m/s and these values should be considered significant and affecting the gear dynamics. The values of the motion parameters obtained in the second simulation are lower than in the first one.



$$z_o = |Ob_1| \sin \varphi_l$$

$$\dot{z}_o = -\dot{\varphi}_a \frac{r_w \tan \varphi_a \sin \varphi_l (\tan^2(\varphi_a) + 1)}{\cos^2 \varphi_l \left( \frac{\tan^2 \varphi_a}{\cos^2 \varphi_l} + 1 \right)^{3/2}}$$

**Analytical equations of kinematic parameters**

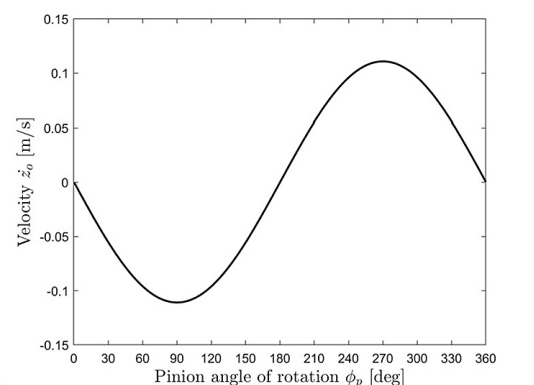
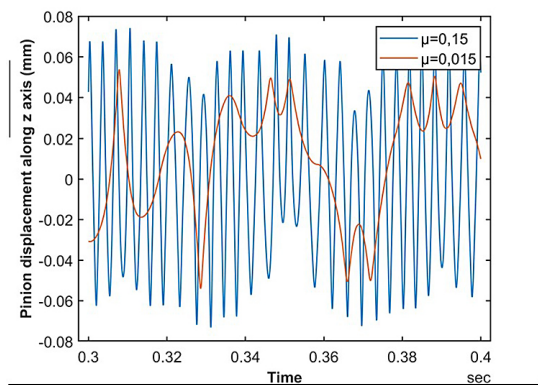
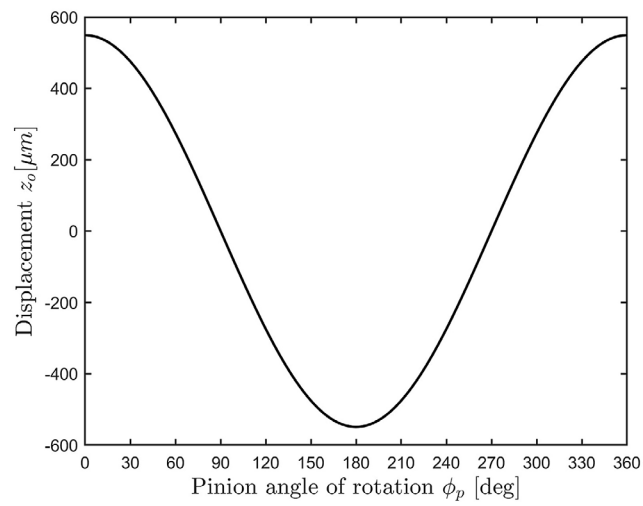
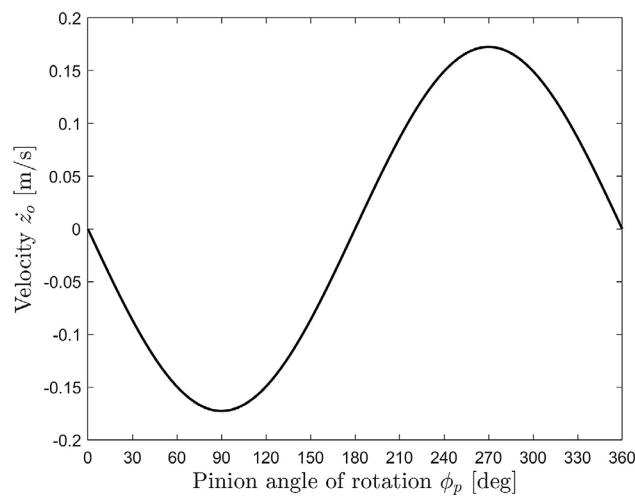


Figure 4. Block diagram



**Figure 5.** Determination of the displacement  $z_o$  for one revolution of the pinion and the angles  $\varphi_{e1} = 0^\circ$ ,  $\varphi_{e2} = 180^\circ$



**Figure 6.** Determination of the velocity  $\dot{z}_o$  for one revolution of the pinion and the angles  $\varphi_{e1} = 0^\circ$ ,  $\varphi_{e2} = 180^\circ$

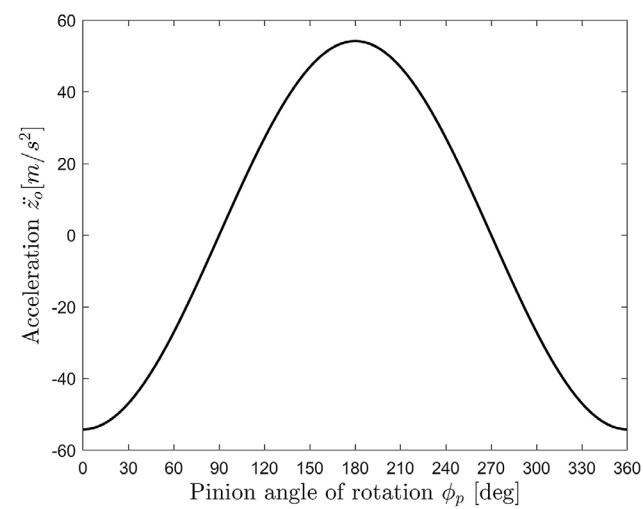


**Figure 7.** Determination of the acceleration  $\ddot{z}_o$  for one revolution of the pinion and the angles  $\varphi_{e1} = 0^\circ$ ,  $\varphi_{e2} = 180^\circ$

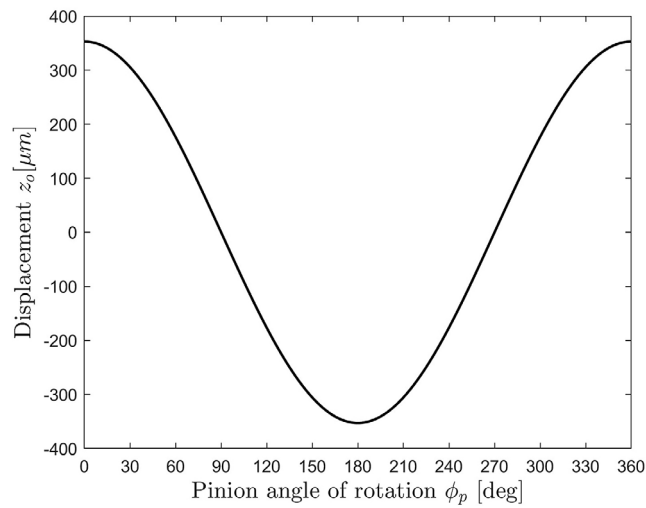


**Figure 8.** Determination of the displacement  $z_o$  for one revolution of the pinion and the angles  $\varphi_{e1} = 50^\circ$ ,  $\varphi_{e2} = 130^\circ$

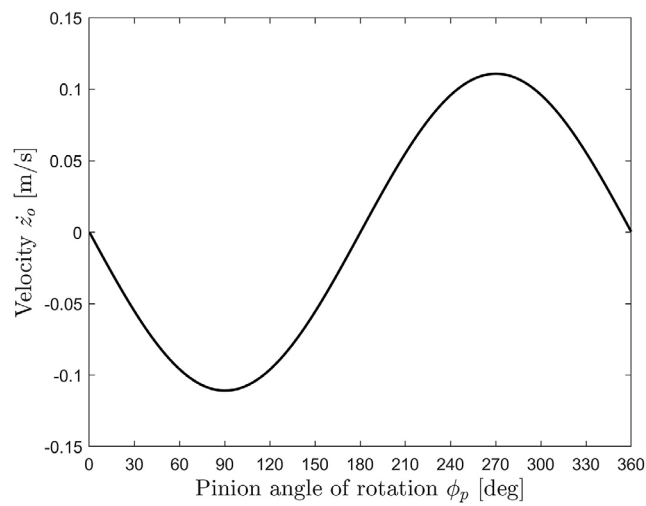


**Figure 9.** Determination of the velocity  $\dot{z}_o$  for one revolution of the pinion and the angles  $\varphi_{e1} = 50^\circ$ ,  $\varphi_{e2} = 130^\circ$

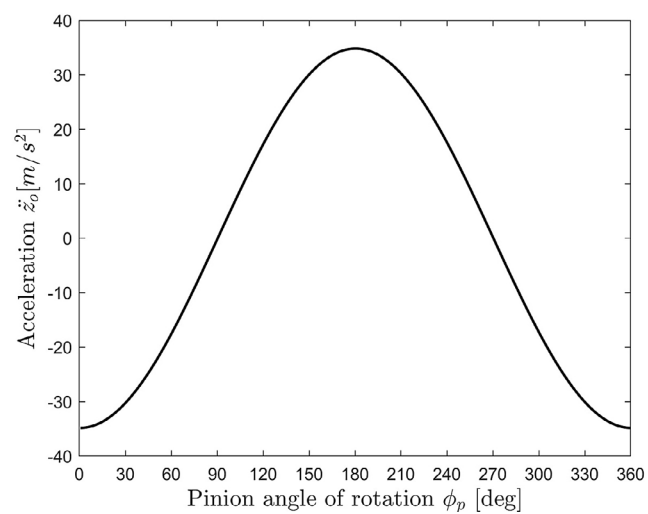


**Figure 10.** Determination of the acceleration  $\ddot{z}_o$  for one revolution of the pinion and the angles  $\varphi_{e1} = 50^\circ$ ,  $\varphi_{e2} = 130^\circ$ .

### ANALYTICAL DYNAMIC MODEL AND SIMULATIONS OF THE OPERATION OF GEARS WITH AXIAL FRICTION

The proposed analytical dynamic model is an extension of the model presented in [17]. Equations 12 and 13 have been added to reflect the degrees of freedom associated with the movement of the shafts along the z-axis of rotation. For this case, parameters like contact ratio and centre distance are dependent on the pinion angle of rotation, and not on time as in previous simulations.

In spur gears, bearings are used for carrying transverse loads. These are usually ball bearings or cylindrical bearings. In this study, ball bearings were assumed. Ball bearings can carry axial loads to a small extent. They are designed such that the radial backlash is small and consistent with the bearing size and type, while the axial backlash is greater than the radial one. Based on previous studies [21] and measurements, the total backlash was set equal to 0.1 mm in the simulation. The backlash model was consistent with that presented in [17].

The equations of axial motion:

$$m_p \ddot{z}_{pCOM} + F_{b12z} = F_{fz} \tag{12}$$

$$m_g \ddot{z}_{gCOM} + F_{b33z} = F_{fz} \tag{13}$$

where:  $F_{fz}$  is the friction force acting along the z-axis (along the axis of shaft rotation),  $F_{b12z}$  is the reaction force of bearings 1 and 2.

Mesh friction was described by a simplified Coulomb friction model. The resultant friction force was divided into two directions: along OLOA and along the z-axis of rotation. The total friction force was maintained constant and equal to the product of the friction coefficient and the contact force. The basic parameters used in the simulation were as follows:

- eccentricity radii  $r_{e1} = r_{e2} = 0.3$  mm,
- eccentricity angles  $\varphi_{e1} = 0^\circ, \varphi_{e2} = 180^\circ$ ,
- backlash  $b_{bz} = 0.1$  mm,
- friction coefficient  $\mu = 0.015$ .

In the second simulation, the friction coefficient value was changed to  $\mu = 0.15$ . Obtained results are plotted, showing the time variations of a given variable, its RMS and maximum values. The variables were the pinion displacement and the friction force along the z-axis.

Figure 11 shows the results of pinion displacement in a function of time. An increase in the friction coefficient causes an increase in the vibration frequency, and the pinion movement becomes more regular.

An analysis of the data in Figure 12 reveals that the maximum value of displacement from the equilibrium position for the friction coefficient  $\mu = 0.015$  is 0.054 mm, while for the friction coefficient  $\mu = 0.15$  it is equal to 0.074 mm. The change in the displacement value is much smaller than that obtained for the friction coefficient, which results from the assumed backlash. The RMS values are 0.029 mm and 0.039 mm, respectively.

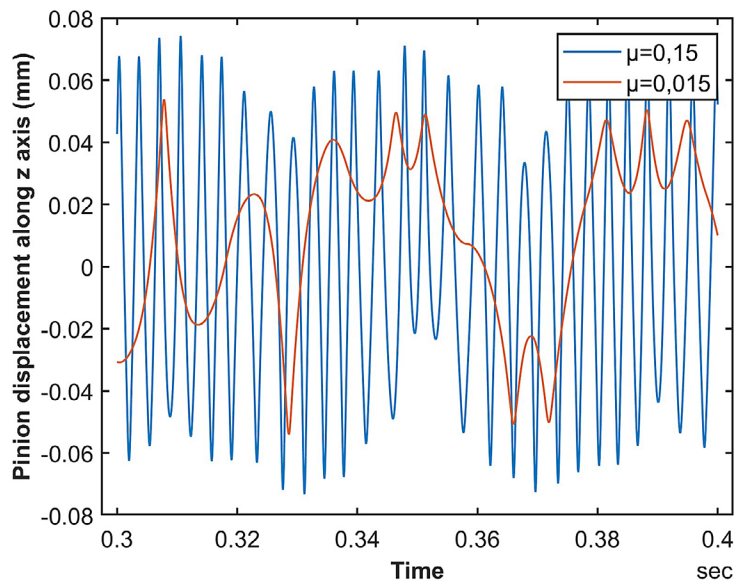


Figure 11. Displacement of a pinion along the z-axis for different friction coefficients

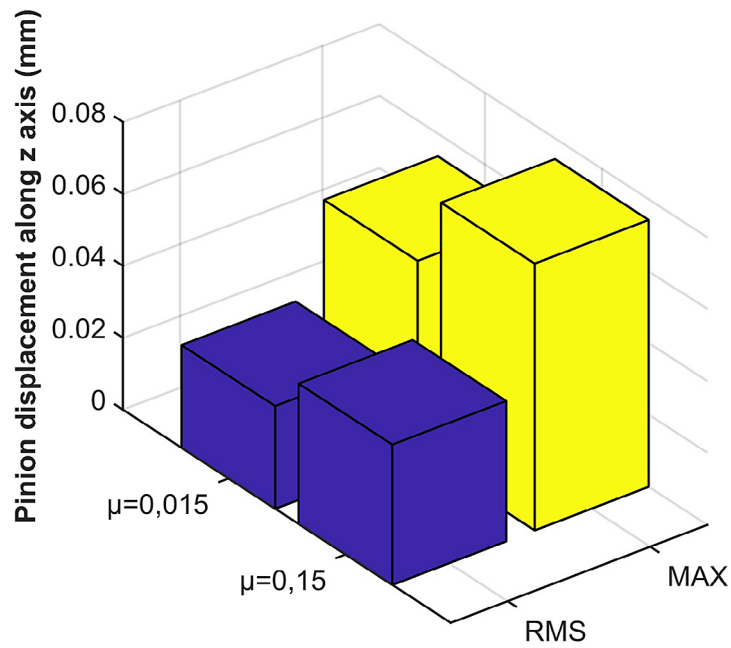


Figure 12. Comparison of RMS and max values for pinion displacement along the z axis

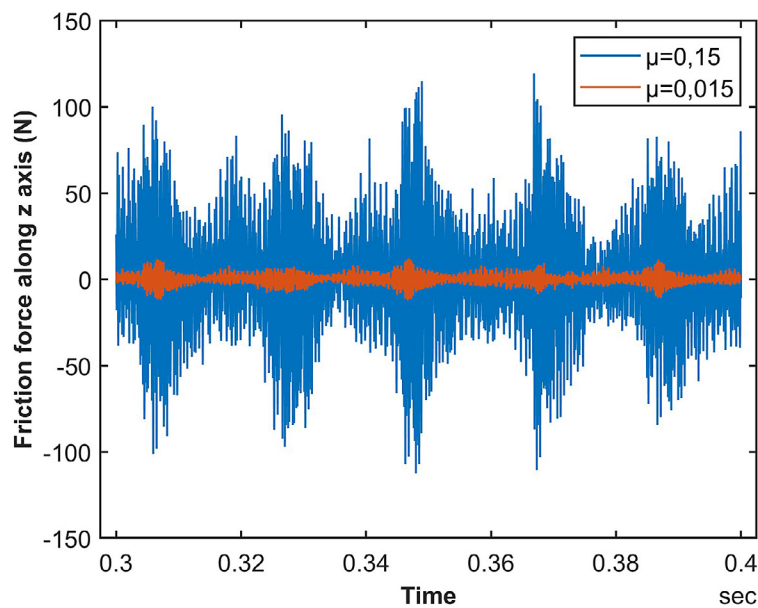


Figure 13. Friction force along the z-axis

The friction force as a function of time is plotted in Figure 13. This is a component of the friction force in the z-axis direction corresponding to the pinion’s axis of rotation. The effect of the friction coefficient value on the friction force is very significant.

The maximum friction force is 12 N for the friction coefficient  $\mu = 0.015$  and 119 N for the friction coefficient  $\mu = 0.15$  (Figure 14). The RMS value is 3 N and 31 N, respectively. These results are as expected, and the friction force is directly

proportional to the friction coefficient. The frequency of variations in the friction force depends on the pinion rotational speed and the direction of z-axis displacement.

## CONCLUSIONS

The main objective of the study was to develop an analytical model that would allow considering gear teeth movement along the axis of

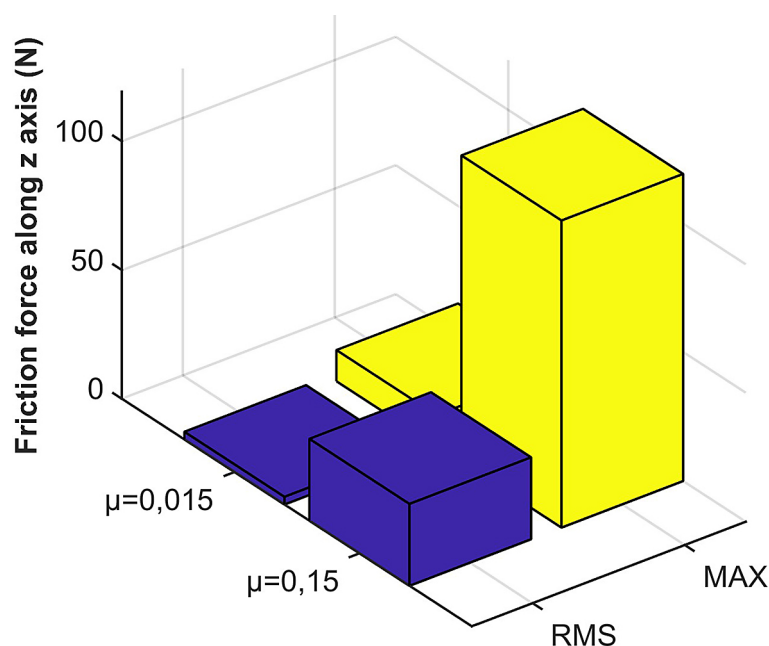


Figure 14. Comparison of RMS and max. value for friction force along the z-axis

rotation for a case of general eccentricity with non-parallel axes. In Sections 3 and 4, numerical simulations were performed to validate the derived relationships and developed models.

Detailed conclusions are as follows:

- It should be noted that the axial movement parameters depend on two main factors, namely the rolling diameter of the gear and the angle  $\varphi_l$ . In turn, the  $\varphi_l$  angle depends on the centre distance and the value and position of eccentricity. The effect of the axial displacement of the gear will be much greater for helical gears and will directly affect the contact point position due to the tooth profile shape. Consequently, the gear ratio error will increase, which will translate into increased vibration and noise.
- The occurrence of axial motion significantly alters the impact of the friction force. In the absence of eccentricity and for a case of eccentricity with parallel axes, the friction force only occurs along the OLOA direction. For eccentricity with non-parallel axes, the friction force can be divided into two force components: the first one acting along the OLOA direction and the other along the axis of gear rotation (in simplified terms). Assuming the Coulomb friction model, this results in a twofold reduction in the value of the component along the OLOA, as the total value of the friction force will not change. In addition, the changes in the senses of the friction

force components occur at different times (for which case the value equals zero), resulting in a sudden increase in one component. A description of the friction force becomes even more complicated. The models which investigate the effect of friction on gear dynamics without taking the axial movement of gear teeth into consideration will not describe the occurring phenomena correctly, as there will be additional axial movement of the gears and shafts caused by the friction force.

The results of this study can serve as a basis for further research into gears, where the effect of gear eccentricity cannot be ignored. Future work will be carried out to investigate other phenomena that are present in the case of gear eccentricity with non-parallel axes.

## REFERENCES

1. Li H., Tang J., Chen S., Ding H., Sun Z., Rong K. Analytical calculation of mesh stiffness for spiral bevel gears with an improved global tooth deformation model, *Mech. Mach. Theory.* 2024; 191. <https://doi.org/10.1016/j.mechmachtheory.2023.105492>
2. Dai H., Long X., Chen F., Xun C. An improved analytical model for gear mesh stiffness calculation, *Mech. Mach. Theory.* 2021; 159: 104262. <https://doi.org/10.1016/j.mechmachtheory.2021.104262>
3. Pedrero J.I., Sánchez M.B., Pleguezuelos M.

- Analytical model of meshing stiffness, load sharing, and transmission error for internal spur gears with profile modification, *Mech. Mach. Theory.* 2024; 197. <https://doi.org/10.1016/j.mechmachtheory.2024.105650>
4. Zheng X., Hu Y., He Z., Xiao Y., Zhang X. On the extended tooth contact and nonlinear dynamics for spur gears—An analytical model, *Mech. Mach. Theory.* 2022; 175. <https://doi.org/10.1016/j.mechmachtheory.2022.104958>
  5. Zheng X., Luo W., Hu Y., He Z., Wang S. Study on the mesh stiffness and nonlinear dynamics accounting for centrifugal effect of high-speed spur gears, *Mech. Mach. Theory.* 2022; 170: 104686. <https://doi.org/10.1016/j.mechmachtheory.2021.104686>
  6. Zheng X., Luo W., Hu Y., He Z., Wang S. Analytical approach to mesh stiffness modeling of high-speed spur gears, *Int. J. Mech. Sci.* 2022; 224. <https://doi.org/10.1016/j.ijmecsci.2022.107318>
  7. Yang L., Wang L., Shao Y., Gu F., Ball A., Mba D. A double-layer iterative analytical model for mesh stiffness and load distribution of early-stage cracked gear based on the slicing method, *Mech. Syst. Signal Process.* 2023; 198. <https://doi.org/10.1016/j.ymsp.2023.110456>
  8. Ning J., Chen Z., Wang Y., Li Y., Zhai W. Vibration feature of spur gear transmission with non-uniform depth distribution of tooth root crack along tooth width, *Eng. Fail. Anal.* 2021; 129: 105713. <https://doi.org/10.1016/j.engfailanal.2021.105713>
  9. Jin Y., Zhang Q., Chen Y., Zu T. A shape-independent analytical method for gear mesh stiffness with asymmetric spalling defects, *Sci. Rep.* 2024; 14: 1–19. <https://doi.org/10.1038/s41598-024-66511-1>
  10. Zhang C., Hu Y., Hu Z., Liu Z. FE-analytical slice model and verification test for load distribution analysis and optimization of planetary gear train in wind turbine, *Eng. Fail. Anal.* 2024; 162: 108451. <https://doi.org/10.1016/j.engfailanal.2024.108451>
  11. Bednarczyk S., Jankowski L., Krawczyk J. The influence of eccentricity changes on power losses in cycloidal gearing, *Tribologia.* 2019; 285: 19–29. <https://doi.org/10.5604/01.3001.0013.5430>
  12. Li S., Pang R., Liu J. Influence of the eccentricity error on the vibrations of a planetary gear, *J. Vibroengineering.* 2022; 24: 1200–1212. <https://doi.org/10.21595/jve.2021.22169>
  13. Huo G., Iglesias-Santamaria M., Zhang X., Sanchez-Espiga J., Caso-Fernandez E., Jiao Y., Viadero-Rueda F. Influence of eccentricity error on the orbit of a two-stage double-helical compound planetary gear train with different mesh phasing configurations, *Mech. Mach. Theory.* 2024; 196: 105634. <https://doi.org/10.1016/j.mechmachtheory.2024.105634>
  14. Qiang Zhao W., Liu J., Hui Zhao W., Zheng Y. An investigation on vibration features of a gear-bearing system involved pitting faults considering effect of eccentricity and friction, *Eng. Fail. Anal.* 2022; 131105837. <https://doi.org/10.1016/j.engfailanal.2021.105837>
  15. Zhao B., Huangfu Y., Ma H., Zhao Z., Wang K. The influence of the geometric eccentricity on the dynamic behaviors of helical gear systems, *Eng. Fail. Anal.* 2020; 118: 104907. <https://doi.org/10.1016/j.engfailanal.2020.104907>
  16. Duan L., Wang L., Du W., Shao Y., Chen Z. Analytical method for time-varying meshing stiffness and dynamic responses of modified spur gears considering pitch deviation and geometric eccentricity, *Mech. Syst. Signal Process.* 2024; 218: 111590. <https://doi.org/10.1016/j.ymsp.2024.111590>
  17. Jedliński Ł. Influence of gear eccentricity with non-parallel axis on the dynamic behaviour of a gear unit using a gear slice model with 26 degrees of freedom, *Adv. Sci. Technol. Res. J.* 2024; 18: 88–102. <https://doi.org/10.12913/22998624/183611>